Stability of Vortex Shedding Modes in the Wake of a Ring at Low Reynolds Numbers

T. Leweke, M. Provansal, and L. Boyer
Laboratoire de Recherche en Combustion, Université de Provence, Centre de Saint-Jérôme, Service 252, F-13397 Marseille Cedex 20, France
(Received 7 June 1993)

The vortex street behind a ring of circular cross section and large aspect ratio is investigated experimentally. Different modes of annular and helical vortex shedding are identified by phase and frequency measurements. Their stability domains overlap in a large interval in Reynolds number where mode selection depends on initial conditions only. A new instability of the vortex shedding process involving characteristic mode transitions has been observed. This instability can be explained in the context of a Ginzburg-Landau model by a mechanism resembling formally the Eckhaus instability of spatially periodic patterns.

PACS numbers: 47.20.Ft, 47.20.Lz, 47.27.Cn, 47.27.Vf

The wake behind a circular cylinder, placed perpendicular to a uniform stream, is generally considered as a reference system for the study of the transition to turbulence in open flows. In recent years, much effort has been put into the investigation of the first step of this transition, the laminar vortex shedding at low Reynolds numbers, known as the Kármán vortex street. We have shown experimentally in 1984 that this Bénard–von Kármán instability can be modeled near the threshold by a Stuart-Landau equation [1]. This was the first application of such an amplitude equation to an open flow system. More recently we extended this model to three-dimensional effects by using a complex Ginzburg-Landau (GL) equation [2,3]. Experimental studies [4–8] had shown the importance of 3D effects—shedding of parallel, inclined, or curved vortices, spanwise cells of different shedding frequencies, or dislocations. It had been found that end effects, always present in experiments, are not negligible, even for long cylinders, and that they are responsible for most of the observed three dimensionalities. The predictions of the GL model are in good agreement with these experimental findings. This strong influence of the end conditions on the vortex shedding led us to investigate the wake of a ring, i.e., a bluff body of circular cross section, but without any ends. In this Letter, we present quantitative experimental results concerning the regime of laminar vortex shedding behind a ring and an interpretation in the frame of the Ginzburg-Landau model.

The experiments were carried out in a small low speed wind tunnel, having a $25\times25\times100$ cm^3 test section. The uniformity of the incoming flow was better than 0.5% and its turbulence level close to 0.1%. The ring, made of brass with a nickel coating to ensure a smooth surface, has a mean diameter $D=56.9$ mm and a thickness $d=3.03$ mm (aspect ratio $\pi D/d=59.0$). It was held in a plane perpendicular to the flow at 15 cm from the entry of the test section by four metal wires of diameter 0.08 mm, tightened by weights. Vibrations were monitored by a sensitive laser-photodiode setup and it turned out that they did not interfere with the flow phenomena in the wake. Velocity measurements were made using two hot wire sensors and a computer controlled mobile laser Doppler anemometer (LDA). Visualizations were obtained with the help of a circular smoke wire placed upstream of the ring. The Reynolds number $\mathrm{Re}=Ud/\nu$ is based on the free stream velocity U and the ring thickness d, ν being the cinematic viscosity of the fluid. Cylindrical coordinates (x,r,φ), with the origin at the center of symmetry of the ring and the x axis pointing in the downstream direction, will be used in the following.

Because of the periodic boundary conditions in the spanwise direction φ and the rotational symmetry of the flow problem, several different vortex configurations are possible: an array of counterrotating vortex rings (observed in Refs. [9–11]) and pairs of counterrotating helical vortices with discrete helix steps of $n\lambda$, where n is an integer and λ the streamwise wavelength of the vortex street. Early evidence of a mode with $n=1$ in the wake of a torus was given by Monson [9], and the existence of

(a)

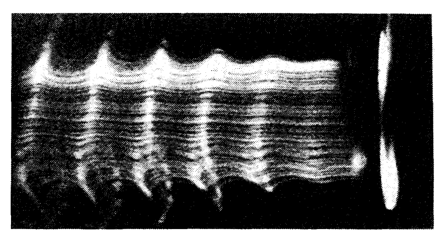

(b)

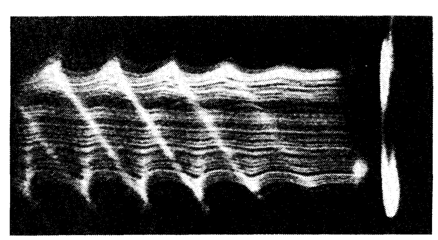

FIG. 1. Visualizations of isophase lines in the wake of a ring of aspect ratio $\pi D/d=59.0$ at $\mathrm{Re}=108$, corresponding to (a) inclined vortex rings and (b) helical vortices of step 2λ. Flow is from right to left.

0031-9007/93/71(21)/3469(4)$06.00

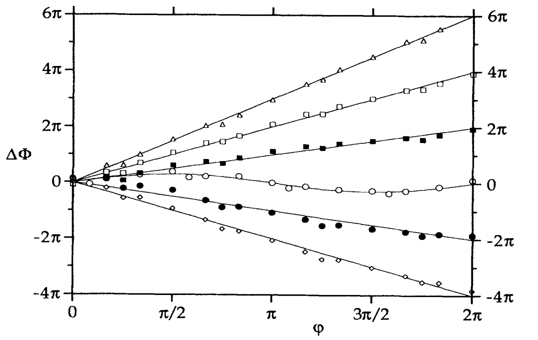

FIG. 2. Spanwise phase variation of the longitudinal velocity fluctuation v_x in the ring wake for different modes at Re = 127. $\Delta\Phi = \arg[v_x(x_0,r_0,\varphi)] - \arg[v_x(x_0,r_0,0)]$, with $x_0 = 3.96d$, $r_0 = D/2 + 0.83d$. Mode labels as in Fig. 4.

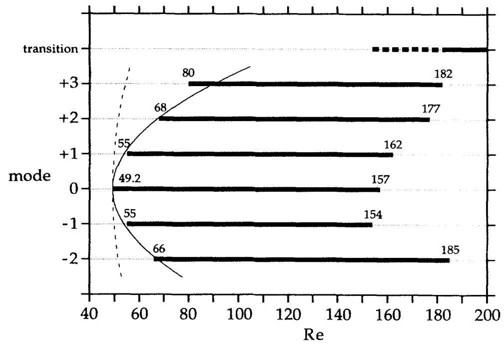

FIG. 3. Domains of stability of the different shedding modes (▬▬), with marginal stability limit (---) and "formation region stability" limit (——), using Eq. (3) with $\mathrm{Re}_0 = 49.2$, $\mu/\nu = 10$, $k = 0.2$, $c_1 = -0.6$, $c_2 = -3.0$.

higher order modes was shown by Leweke, Provansal, and Boyer [12]. Visualizations of two modes observed in the present experiments can be seen in Fig. 1. The different modes can be characterized by the variation in the spanwise direction of the phase Φ of the time-periodic velocity fluctuations in the wake. The phase difference $\Delta\Phi(\varphi) = \Phi(\varphi) - \Phi(0)$ was obtained for a series of φ from the correlation function of the simultaneous velocity signals from the mobile LDA point and a fixed hot wire serving as a phase reference (see also caption of Fig. 2). Figure 2 shows $\Delta\Phi(\varphi)$ for all the modes observed in the present configuration, from $n = -2$ to $+3$. The wake for $n = 3$ consists of *six* interwoven helical vortices. The almost sinusoidal phase variation of the mode 0 results from the slight inclination of the vortex rings with respect to the body.

It has to be pointed out that each mode is stable in a large domain in Reynolds number, as visible in Fig. 3, and that between Re = 80 and 154 all modes are possible. The mode selection in regions where several modes can exist depends only on initial conditions. In the experiments, modes could be forced with a reasonable repeatability by short but violent transverse perturbations of the incoming flow, created by means of strong air jets. The fact that the mode $n = -3$ or modes with even higher $|n|$ were not observed in the present experiments may be due to the difficulty of creating suitable initial conditions.

It is known from experiments on circular cylinder wakes (see, e.g., [6]) that the shedding frequency f at a given Reynolds number is a function of the shedding angle θ. The same behavior is observed in the ring wake. The Strouhal number $S = fd/U$ was determined as a function of the Reynolds number for all the modes in the laminar regime using a hot wire and a standard spectrum analyzer to determine f. The result is shown in Fig. 4(a). The Strouhal number decreases with increasing mode number $|n|$, i.e., with increasing shedding angle. It is worth noticing that the frequency laws of all the laminar modes are continuous due to the absence of end effects, which could cause discontinuities in the S-Re relationship in the case of a circular cylinder [6,7].

Figure 4(b) shows the same data after application of the transformation $S \to S/\cos\theta$ used by Williamson [6] and which is, to a good approximation, also included in the Ginzburg-Landau model [2]. As in the case of a straight cylinder the transformed frequency laws of the ring wake collapse to one single curve, despite the presence of a body curvature. The mean shedding angle θ used for the transformation was obtained from the streamwise wavelength λ of the wake, which had been

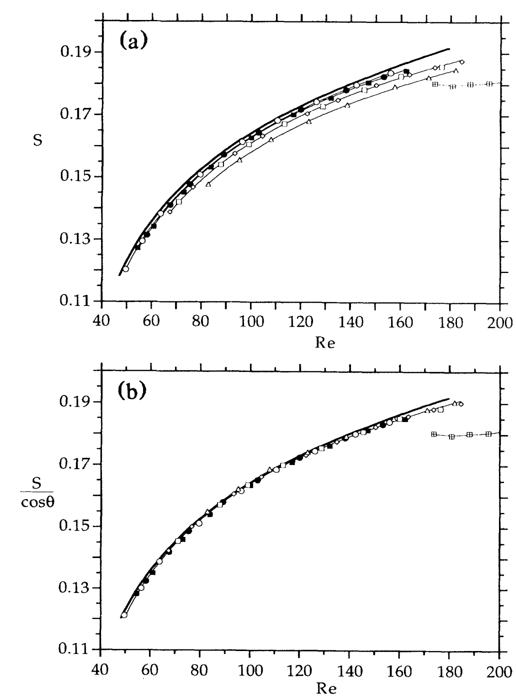

FIG. 4. Frequency laws: Strouhal number S vs Reynolds number Re, (a) as measured and (b) transformed by the $\cos\theta$ law. Modes: ○: 0; ■: +1; ●: −1; □: +2; ◇: −2; △: +3; ⊞: transition; ——: parallel shedding behind a straight cylinder (from [6]).

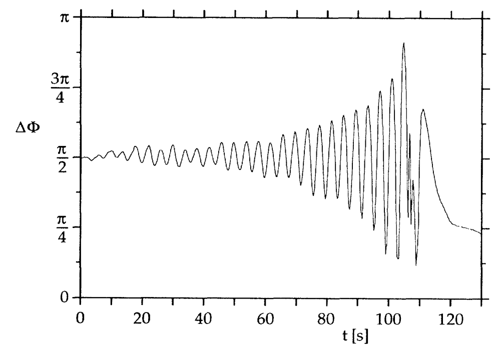

FIG. 5. Transition from mode -2 to mode 0 after a change in Reynolds number from Re$=66.6$ to 65.2 at $t=0$: time evolution of the difference $\Delta\Phi$ between the phases of the longitudinal velocity fluctuation at two points in the wake, chosen to have $\Delta\Phi(t=0)=\pi/2$ for reasons of signal processing.

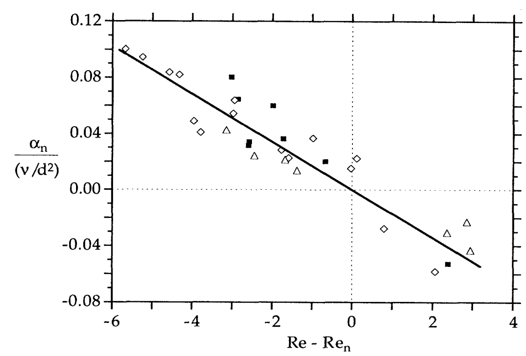

FIG. 6. Growth rate α_n of the instability of the helical vortex patterns, determined from measurements as in Fig. 5. Negative growth rates were found by letting the instability grow with Re $<$ Re$_n$ and by switching to Re $>$ Re$_n$ before the initial mode broke down. Labels of the initial mode as in Fig. 4.

measured as a function of Re for all the modes. For the helical modes, the helix angle $\theta=\tan^{-1}(n\lambda/\pi D)$ is used. For the inclined vortex ring mode, the shedding angle varies approximately as $\sin(\varphi-\varphi_0)$ (see Fig. 2). For this mode we use a mean absolute value of θ given by $\theta=\tan^{-1}[\lambda(\Delta\Phi_{\max}-\Delta\Phi_{\min})/\pi^2 D]$.

Figure 4(b) shows that the frequencies of parallel shedding behind the ring seem to be slightly lower than in the case of a straight cylinder, a feature already noticed by Roshko [13]. However, the differences between the two curves are of the same order as the experimental uncertainties.

When increasing the Reynolds number, the higher order helix modes show a tendency to remain stable longer than the lower order or vortex ring modes. When passing the upper Re stability limit in a low order mode, the wake switches abruptly to a transition mode, characterized by a loss of the wake periodicity and a less pronounced peak in the velocity spectra. In the range between Re$=154$ and 185, the wake then stays in this mode during a random time interval before restabilizing in a higher order mode which is still stable at the new Reynolds number.

When decreasing Re, the helix modes become unstable below a critical Reynolds number Re$_n$, which itself increases with $|n|$. The transition of a helix mode n to a new configuration when passing its stability limit Re$_n$ happens in a very characteristic way. This is illustrated for the transition $-2\rightarrow 0$ in Fig. 5 where the evolution of the phase difference $\Delta\Phi$ of the velocity at two points in the wake after a step change in Re from above to below critical is shown. $\Delta\Phi$ was obtained from the signals of two fixed hot wires and an analog phase meter. After the change in Re the phase difference, initially a constant, begins to oscillate with an exponentially growing amplitude until the initial mode breaks down and the wake reorganizes in a different mode with lower $|n|$ and a phase difference which is again a constant. It is worth noting the time scales involved. For the case shown in Fig. 5 the transition takes about 2 min, i.e., almost 2000 shedding cycles in the present case. During this process, the amplitude of the *velocity* oscillation remains practically unchanged. At the same time the velocity spectra exhibit sideband peaks at the combinations between the Kármán and phase fluctuation frequencies. The latter is of the same order of magnitude as the differences between Kármán frequencies of the modes at the given Re. Within the limits of experimental uncertainty, the linear growth rate of the fluctuations is proportional to the threshold deviation Re$-$Re$_n$, as shown in Fig. 6. The slope is almost the same for the transitions of three different helical modes. The same behavior is observed for the phase difference between any two points in the wake.

These mode transitions and the associated stability limits can be understood in the framework of the phenomenological Ginzburg-Landau model mentioned above. In this model, the wake formation region is represented by a one-dimensional array of diffusively coupled nonlinear oscillators distributed along the spanwise direction of the body (φ for the torus). The wake pattern is obtained by relating the downstream direction x to time t using the transformation $t\rightarrow -x/U_c$, where U_c is the convection speed of the vortices. It must be emphasized that the GL model is used for modeling diffusive processes along the *spanwise* direction; it does not contain any dependence on the downstream coordinate. This model has been successful in describing 3D effects in the wake of cylinders [2,3] and also rings [12]. For the ring, the following complex GL equation is used:

$$\frac{\partial A}{\partial t}=\sigma(1+ic_0)A+\mu(1+ic_1)\frac{\partial^2 A}{\partial(D\varphi/2)^2}-l(1+ic_2)|A|^2A\,, \qquad (1)$$

with periodic boundary conditions in the spanwise direction φ:

$$A(\varphi=0,t)=A(\varphi=2\pi,t)\,. \qquad (2)$$

A is the complex amplitude of the velocity fluctuations,

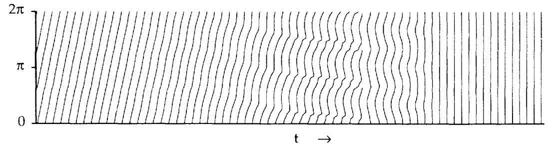

FIG. 7. Numerical simulation of the ring wake using Eqs. (1) and (2) with Re=65, $k=0.2$, $\mu=10\nu$, $l=25/\nu$, $c_0=11.8$, $c_1=-0.5$, $c_2=-4.0$, and mode 3 as initial condition. This spatiotemporal plot of isophase lines of A corresponds to a wake visualization, with the body on the right-hand side and flow from right to left. The transition is very rapid because of the great threshold deviation ($\mathrm{Re}-\mathrm{Re}_3 \approx -42$).

$\sigma=k(\nu/d^2)(\mathrm{Re}-\mathrm{Re}_0)$, and k, μ, l, c_0, c_1, and c_2 are model parameters (see Refs. [2,12]). The "plane wave" solutions of Eq. (1), which, because of (2), have discrete spanwise wave numbers, correspond to the different modes observed experimentally in the ring wake. These waves exhibit an instability with respect to long wavelength disturbances for wave numbers (i.e., shedding angles) above a certain limit, which is a function of Re [3,14]. The analytic treatment [14] predicts instability for

$$\mathrm{Re} < \mathrm{Re}_n = \mathrm{Re}_0 + \frac{4(\mu/\nu)}{k(D/d)^2}\left[\frac{3+c_1c_2+2c_2^2}{1+c_1c_2}\right]n^2 . \qquad (3)$$

In this expression finite size effects due to the periodic (and not infinite) domain are neglected. A calculation analogous to the one discussed in Refs. [15,16] for the complex GL equation shows that in our case these effects are smaller than the experimental uncertainty. The stability limit $\mathrm{Re}_n(n)$ is plotted in Fig. 3 as a continuous line. The model constants, chosen empirically, are consistent with previous measurements in cylinder wakes (see Refs. [2,3]). The dashed line in Fig. 3 corresponds to the marginal curve of oblique shedding with zero amplitude.

Figure 7 shows the result of a numerical simulation of the GL model equation representing a visualization of the wake. The phase fluctuations of Fig. 5 correspond to a growing waviness of the vortices (see also Ref. [2]). The breakdown of the initial mode occurs via vortex dislocations. The pattern in Fig. 7 produces the same kind of phase fluctuations and "velocity" spectra as in the experiments.

Figure 3 resembles strongly the stability diagrams encountered in thin-layer cellular convection [15,16], where similar GL model equations are used to describe the spatial patterns and where the instability corresponding to the one presented here is known as the Eckhaus instability. This resemblance is purely mathematical: In the present case we are *not* dealing with an instability of the periodic streamwise vortex pattern in the wake, but an instability of the *spanwise structure of the vortex formation and shedding process.* The waviness of the vortices resulting from this near wake instability must also be distinguished from the waves associated with far wake instabilities observed, e.g., by Cimbala, Nagib, and Roshko [17].

To our knowledge, this is the first experimental evidence of such a kind of instability in open flows. Since the GL model does not incorporate the body curvature, this instability should also appear in the wake of circular cylinders, and it may be at the origin of the cell formation observed by König, Eisenlohr, and Eckelmann [7] or the transition between oblique shedding modes seen by Williamson [6]. The ring geometry, however, with its discrete shedding angles and the absence of end effects influencing the whole wake, seems to be more convenient for the experimental observation of this instability in bluff body wakes at low Reynolds numbers.

The authors wish to thank P. Albarède, C. H. K. Williamson, P. Pelcé, and A. Pocheau for many helpful discussions. We are also grateful to J. Minelli and F. Abetino for their technical assistance. This work is supported by the French CNRS as part of the Groupement de Recherche "Ordre et Chaos dans la Matière" and by the European Community under Contract No. JOU2-CT92-0159. Laboratoire de Recherche en Combustion is CNRS URA No. 1117.

[1] C. Mathis, M. Provansal, and L. Boyer, J. Phys. (Paris), Lett. **45**, L483 (1984).
[2] P. Albarède, thesis, Université de Provence, Marseille, France, 1991.
[3] P. Albarède and P. A. Monkewitz, Phys. Fluids A **4**, 744 (1992).
[4] E. Berger and R. Wille, Annu. Rev. Fluid Mech. **4**, 313 (1972).
[5] M. Provansal, C. Mathis, and L. Boyer, J. Fluid Mech. **182**, 1 (1987).
[6] C. H. K. Williamson, J. Fluid Mech. **206**, 579 (1989).
[7] M. König, H. Eisenlohr, and H. Eckelmann, Phys. Fluids A **2**, 1607 (1990).
[8] M. Hammache and M. Gharib, J. Fluid Mech. **232**, 567 (1991).
[9] D. R. Monson, Trans. ASME, J. Fluids Eng. **105**, 308 (1985).
[10] M. Takamoto, Bull. NRLM (Japan) **36**, Suppl. No. 139 (1987).
[11] P. W. Bearman and M. Takamoto, Fluid Dyn. Res. **3**, 214 (1988).
[12] T. Leweke, M. Provansal, and L. Boyer, C.R. Acad. Sci. Paris **316**, Sér. II, 287 (1993).
[13] A. Roshko, NACA Report No. 1191, 1954 (unpublished).
[14] Y. Kuramoto, *Chemical Oscillations, Waves, and Turbulence* (Springer-Verlag, Berlin, 1984).
[15] L. Tuckerman and D. Barkley, Physica (Amsterdam) **46D**, 57 (1991).
[16] L. Kramer and W. Zimmermann, Physica (Amsterdam) **16D**, 221 (1985).
[17] J. M. Cimbala, H. M. Nagib, and A. Roshko, J. Fluid Mech. **190**, 265 (1988).

(a)

(b)

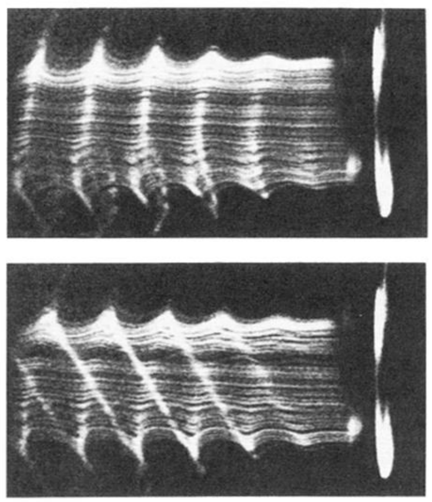

FIG. 1. Visualizations of isophase lines in the wake of a ring of aspect ratio $\pi D/d = 59.0$ at $\mathrm{Re} = 108$, corresponding to (a) inclined vortex rings and (b) helical vortices of step 2λ. Flow is from right to left.